IEEE/CSC & ESAS SUPERCONDUCTIVITY NEWS FORUM (global edition), January 2016.
EUCAS 2015 preprint 2A-M-P-02.03. Submitted to *IEEE Trans. Appl. Supercond.* for possible publication.

Direct Measurements of Field-Dependent Ordering in a Low-Field Vortex Glass State

Frederick S. Wells, Alexey V. Pan, X. Renshaw Wang, Igor A. Golovchanskiy, Sergey A. Fedoseev, Hans Hilgenkamp, Anatoly Rozenfeld

***Abstract*—The variation of topological defect density and hexatic order parameter were measured over a range of micro-Tesla fields in a two-dimensional superconducting vortex glass. This was achieved through scanning SQUID microscopy of the vortex distribution in $YBa_2Cu_3O_{7-\delta}$ thin films under field-cooled conditions. It was discovered that while the defect density decreased for increasing magnetic fields, giving the impression of a more lattice-like vortex distribution, the hexatic order parameter also decreased, showing that the distribution was less orientationally ordered.**

***Index Terms*—Flux pinning, Superconducting thin films, Yttrium barium copper oxide, Scanning probe microscopy**

I. Introduction

GLASS-LIKE distributions of vortices in type II superconductors have been a subject of intense interest in recent years [1], [2], in both the two-dimensional (thin film) [3] and three dimensional (bulk) [4] cases.

Most studies into vortex glass behaviour involve measurement or simulation of macroscopic quantities such as transport current and sample magnetisation to determine transitions in the vortex phase diagram [3], [4]. Analyses of the properties of vortex glass states by direct measurement are less common, but may provide a more fundamental understanding of the nature of these distributions of vortices [5].

In the absence of defects or thermal fluctuations, the distribution of vortices in a superconductor would be a regular triangular lattice with sixfold rotational symmetry. In this perfect lattice each vortex has six nearest neighbours. However, in reality even highly ordered vortex distributions in the lattice state possess topological defects, which can be dislocations (positional defects) or disclinations (orientational defects) [6], [7]. Ryu and Stroud identify a disclination in the vortex lattice as a vortex having a number of nearest neighbours other than 6, and a dislocation as a pair of adjacent disclinations with one having more nearest neighbours and one having less [7].

The vortex glass state is highly non-regular and dominated by such defects. Superconducting phase diagrams often show a rich variety of glass-like states with complex transition lines [1], [3], [4]. However, in this two-dimensional study we consider only the differences between a hexatic vortex glass, in which a sixfold orientational order is maintained, and an isotropic vortex glass, in which it is not [1], [4], [7].

In this work, the distribution of vortices in low field glass states are directly observed by scanning Superconducting Quantum Interference Device (SQUID) microscopy of $YBa_2Cu_3O_{7-\delta}$ (YBCO) thin films. Scanning SQUID Microscopy (SSM) is a magnetic microscopy technique with very high resolution, sufficient to resolve superconducting vortices [5], [8], [13]. A vortex glass state is expected in YBCO thin films grown by pulsed laser deposition (PLD) due to the high number of strong pinning sites [10]–[12].

From the SSM images, vortex positions were mapped and Delaunay triangulation used to examine the ordering of the vortex glass in terms of distribution of the number of neighbours to each vortex and the hexatic order parameter.

We find that the modal number of nearest neighbours is six for all fields studied, but that the proportion of vortices having six nearest neighbours increases with increasing applied field.

We also find that the angular distribution of vortices becomes less regular for higher fields in the observed field range, evidenced by a decreasing hexatic order parameter.

II. Experimental Details

$YBa_2Cu_3O_{7-x}$ films with thickness close to 200 nm were grown by pulsed laser deposition [14]–[16] on a strontium titanium oxide substrate. The critical temperature (T_c) of the film used was measured to be 90.0 ± 0.5 K using a Quantum Design Magnetic Property Measurement System.

Multiple field-coolings from above T_c to 4.2K were undertaken for the same YBCO film for a range of fields in the low field vortex-glass region of the phase diagram (between 0.05 and 5.47 μT). The distribution of vortices in the film was directly examined for each field once the temperature had stabilised, using the scanning SQUID microscopy (SSM) technique described in [5]. The SQUID loop has size 3 μm $\times$ 5 μm, and nominal scan height of 5 μm.

Manuscript submitted August 23, 2015. This work is supported by the Australian Research Council and the University of Wollongong.

F. S. Wells, A. V. Pan, S. A. Fedoseev and I. A. Golovchanskiy are with the Institute for Superconducting and Electronic Materials, University of Wollongong, Northfields Avenue, Wollongong, NSW 2522, Australia (e-mail: pan@uow.edu.au).

X. R. Wang and H. Hilgenkamp are with the Faculty of Science and Technology and MESA+ Institute for Nanotechnology, University of Twente, P.O. Box 217, 7500 AE Enschede, The Netherlands.

X. R. Wang is with Electrochemical Energy Laboratory, Massachusetts Institute of Technology, Cambridge, MA 02139, USA.

S. A. Fedoseev and A. Rozenfeld are with the Center for Medical Radiation Physics, University of Wollongong, Northfields Avenue, Wollongong, NSW 2522, Australia.

I. A. Golovchanskiy is with the Laboratory of Topological Quantum Phenomena in Superconducting Systems, Moscow Institute of Physics and Technology, State University, 9 Institutskiy per., Dolgoprudny, Moscow Region, 141700, Russia, and the Laboratory of Superconducting Metamaterials, National University of Science and Technology MISIS, 4 Leninsky prosp., Moscow, 119049, Russia.

Current in the samples was calculated from the resulting SSM images using an inverse Biot-Savart law procedure [13], [21]–[23].

The position of vortices in SSM images was determined programmatically using a particle detection algorithm to give an array of spatially distributed vortex locations. Delaunay triangulation was applied to the vortex positions to determine the number of nearest neighbours to each vortex and the bond angle of each of these neighbours.

Delaunay triangulation is a mathematical procedure mapping the distribution of vortices in space to a network of non-overlapping triangles. Each triangle has a vortex at each corner and has edges connecting nearest-neighbouring vortices.

From this triangulation the number of nearest neighbours to each vortex was determined for all internal vortices. Where internal vortices are defined as all vortices excluding those at the edges of the measured area or at the sample edge, as well as their nearest neighbours.

The hexatic order parameter (HOP) was also determined for each vortex distribution. The HOP is given by $|\psi_6|^2$, where:

$$\psi_6 = \frac{1}{N_{int}} \sum_i \frac{1}{n(i)} \sum_j e^{6i\theta_{ij}} \quad (1)$$

Here N_{int} is the number of internal vortices, $n(i)$ is the number of nearest neighbours to a vortex i, θ_{ij} is the angle between nearest-neighbouring vortices i and j relative to a fixed axis.

A regular triangular vortex lattice (as expected for a defect-free superconducting sample) has a sixfold rotational symmetry and hence has hexatic order parameter $|\psi_6|^2 = 1$. Any deviation from the regular lattice reduces the HOP to a value between 1 and 0.

III. Results

Scanning SQUID images were obtained after field cooling at several field values in the specified range. Figure 1 gives typical magnetic field data at a particular field value.

The light region is the superconducting sample, with dark spots showing vortex positions. The dark area at the left is outside the sample. The vortices in this image appear larger than their actual size, and show an apparent asymmetry due to the scan height and angle of the SQUID magnetometer [5].

Current calculated in the film from similar SSM images is shown in figure 2, for scans taken with different field histories.

Vortices are seen here as dark spots since no current flows in the vortex core, with bright circulating currents around. Shielding currents are also seen at the sample edge, especially in the lower-field images.

Delaunay triangulation was applied successfully to the vortex positions from scanning SQUID data at each field, as shown in figure 3.

The number of nearest neighbours to each vortex was calculated by defining nearest-neighbouring vortices as those connected in the same triangle by the triangulation algorithm. That is, any three vortices through which a circle can be drawn which encompasses no other vortices are defined to be neighbours.

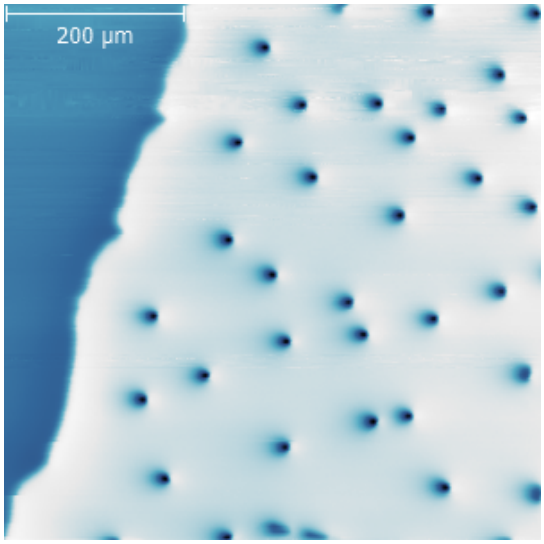

Fig. 1. Scanning SQUID image of vortices near the edge of a YBCO film after field cooling at 1.47 μT. The brightness of each pixel represents the strength of magnetic field at the corresponding point on the sample. The scale bar is 200 μm.

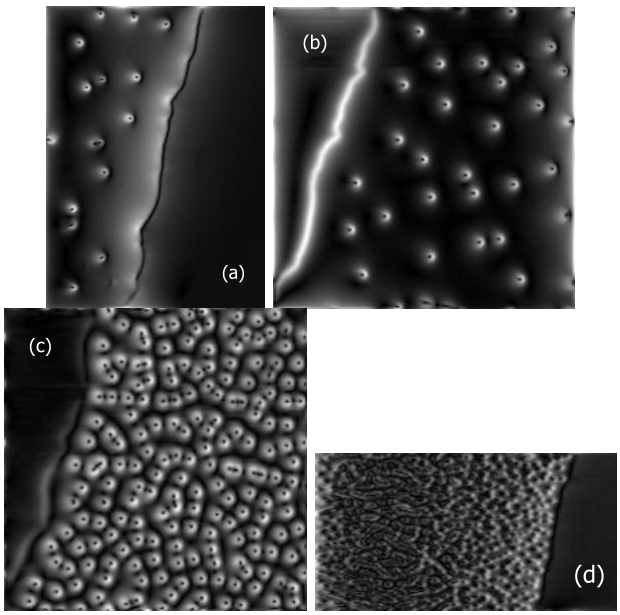

Fig. 2. Current in YBCO film after field cooling at (a) 0.05 μT, (b) 1.47 μT, (c) 2.10 μT and (d) 5.46 μT, calculated from Scanning SQUID images. Brighter regions represent higher currents.

The distribution of the number of nearest neighbours to each internal vortex at a particular field is shown in figure 4(a). A Gaussian fit is plotted for each distribution of vortices, excluding the 1.47 μT scan as it contained only 17 internal vortices and hence the spread of nearest neighbour numbers could not be accurately determined. The 0.05 μT scan is excluded from analysis completely as it contains no internal vortices by the definition given above.

The full width at half maximum (FWHM) of these fit curves represents the spread of the number of nearest neighbours. This width is plotted against field in part (b) of this figure. It is found that the FWHM decreases linearly with applied

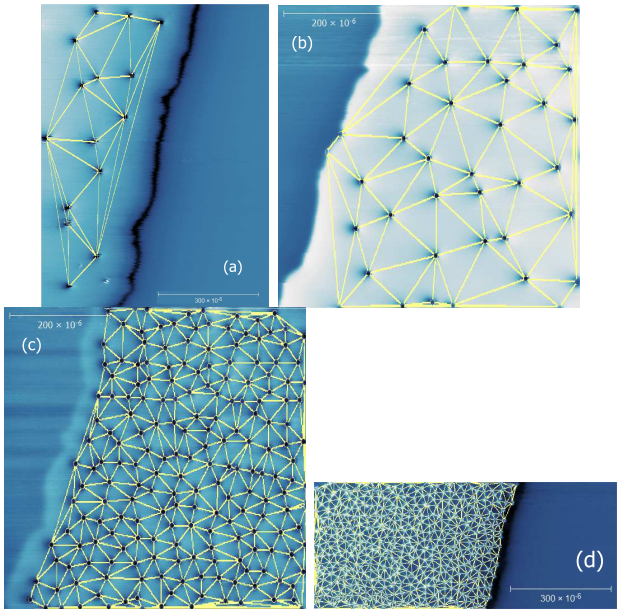

Fig. 3. Delaunay triangulation mapped onto scanning SQUID images at (a) 0.05 μT, (b) 1.47 μT, (c) 2.10 μT and (d) 5.46 μT. Scale bars indicate size in metres. The triangulation is represented by lines connecting each detected vortex position to its neighbours (colour online).

field, but with relatively low gradient. This indicates that for higher fields a greater proportion of vortices have six nearest neighbours, and hence that the number of topological defects (as defined above) slightly decreases with field in the range measured.

The angle between vortices is also measured from the Delaunay triangulation, and this is used to calculate the hexatic order parameter for each field value used. The HOP is plotted against field in figure 5.

It is seen that the HOP decreases with increasing field in an inversely proportional manner. This implies that the angles between vortices become less regular for increasing field in the field range studied.

IV. Discussion

As mentioned previously, significant spread of the magnetic stray field occurs between the sample surface and the scan height, increasing the apparent size of vortices. In some cases this leads to pairs of vortices being indistinguishable from a single vortex in the SSM image. Several groups of vortices with apparent overlap can be seen in figure 7.

To investigate this, linear profiles of measured field were plotted across pairs of closely spaced vortices in the 5.46 μT scan. Figure 6 shows the profiles of pairs of vortices at 13 μm and 9 μm separation, showing that the stray fields from vortices closer than about 10 μm overlap so as to give no point of zero measured field between the vortices.

This overlap causes errors in the analysis of these vortices, most significantly that the particle detection algorithm may falsely recognise two closely-spaced vortices as a single vortex. This then causes error in the number of nearest neighbours to this and surrounding vortices, as well as the angles between these vortices. Both of these errors will in turn affect the hexatic order parameter.

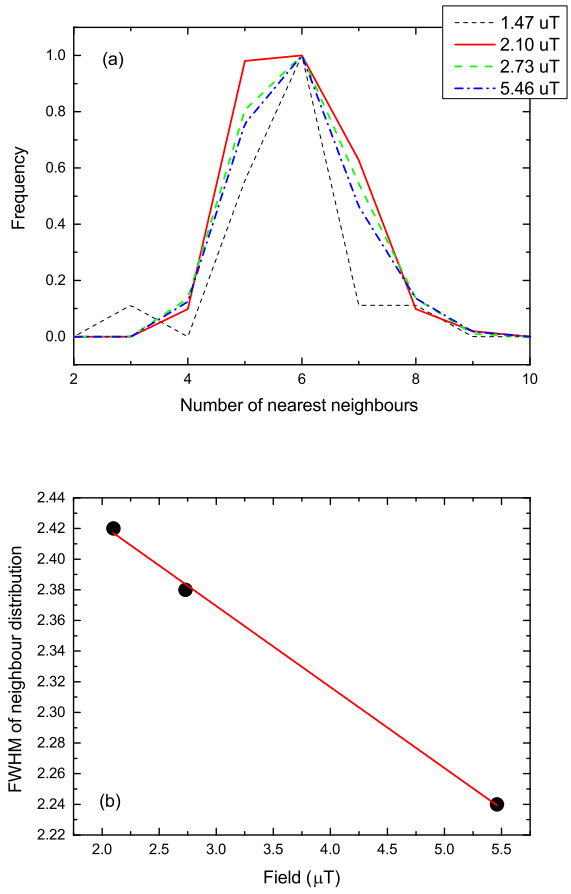

Fig. 4. (a) Normalised occurrence of the number of nearest neighbours to vortices in the SSM scans at fields given in the legend. (b) Plot of the width of the Gaussian fit to these curves against applied field. A linear trend line is plotted with gradient (-5.29 $\pm$ 0.19) $\times 10^4$ T^{-1}.

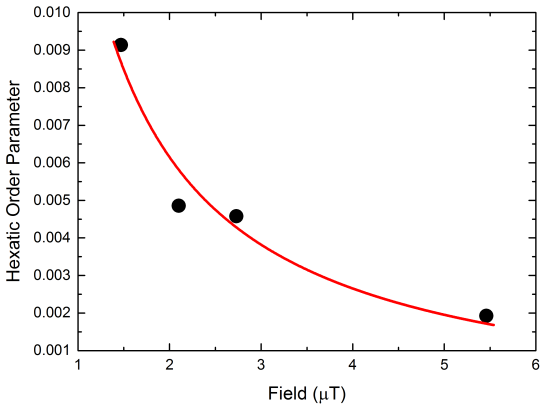

Fig. 5. Variation of the hexatic order parameter $|\psi_6|^2$ with applied field. Values calculated from Delaunay triangulation of vortex positions from scanning SQUID images. The fit curve is hyperbolic, with equation $1/|\psi_6|^2 = B \times (9.99 \pm 0.74) \times 10^7$ T^{-1}.

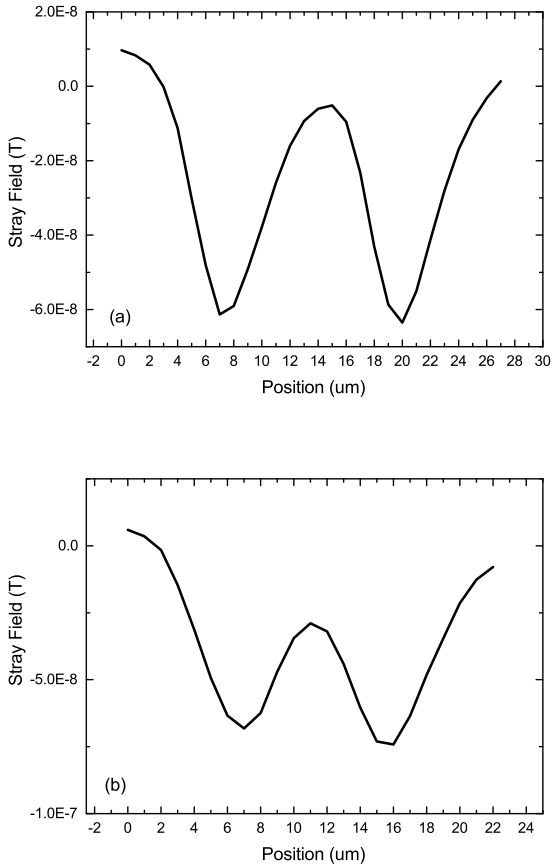

Fig. 6. Field profiles across closely paired vortices showing (a) no stray field overlap at 13 μm separation and (b) half-height overlap at 9 μm separation, which may result in a failure to interpret these as separate vortices.

The particle detection parameters were optimised for each vortex distribution independently in order to avoid such errors, and the Delaunay triangulation was visually examined for false vortex positions after each attempt. By this process all of the distributions were mapped with a high degree of accuracy, except for the 2.73 μT scan, which had lower quality. Therefore the HOP and nearest neighbour data calculated at this field were given lower weighting for trend line calculations.

This scan does however show one interesting feature not seen in other scans: a linear region of notably increased vortex density with length at least 400 μm, as shown in figure 7. This high-density region was seen to be reproduced upon heating above T_c and re-cooling, implying that it is a linear defect with width of the order of the size of vortices or smaller. This may be caused by substrate twinning, an extended grain boundary, or micro-mechanical damage to the sample.

This defect is not seen in other scans as they were taken at different positions on the sample.

V. Conclusion

We have directly examined the field dependence of the ordering of vortices in the low-field vortex glass state in a YBCO thin film, as observed by scanning SQUID microscopy

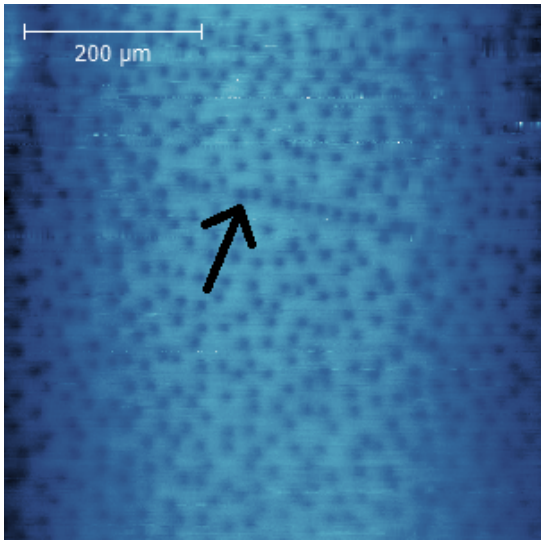

Fig. 7. Scanning SQUID image of vortices in the YBCO film after field cooling at 2.73 μT, showing the presence of a linear defect, as indicated by the arrow.

of field-cooled states. Ordering of the vortex glass is quantified using two parameters: the spread of the number of nearest neighbours to each vortex, and the hexatic order parameter.

While the distribution of nearest neighbours peaked at six for all fields studied, the width of this distribution decreased rather linearly with increasing applied field, but the overall change was slight. This shows that for higher fields, the proportion of vortices having more or less than six nearest neighbours decreases (i.e. the relative number of topological defects decreases), and the vortex distribution becomes slightly more resemblant of a regular triangular lattice.

It was therefore expected that the hexatic order parameter would also increase with increasing field, especially since the influence of vortex-vortex repulsion is heightened for larger fields, thereby moving the sample closer to the vortex lattice region of the phase diagram from the low-field (re-entrant) vortex glass region [2].

However, the opposite was seen from the results. Hexatic order parameter was shown to be inversely proportional to applied field. This shows that while the number of topological defects decreases with increasing field, the angle between vortices is less regular and orientational order is overall decreased.

If the same study were continued to higher fields, we expect that the vortex distribution would transition into the lattice state at some well-defined point [24], [25]. The hexatic order parameter would be expected to reach a minimum before increasing sharply at the vortex glass-lattice transition, while the number of topological defects should decrease steadily before sharply dropping at this transition point [7]. The HOP and nearest neighbour distribution may also vary with field in the vortex lattice regime, and may have different field dependences in the high-field vortex glass phase and in other glass-like phases.

Direct measurements of field-dependant vortex ordering in other regions of the phase diagram may prove to be a very exciting avenue for future research.

REFERENCES

[1] T. Natterman, S. Scheidl (2000) "Vortex-Glass Phases in Type-II Superconductors" *Adv. Phys.* **49** 607.

[2] D.S. Fisher, M.P.A. Fisher, D.A. Huse (1991) "Thermal Fluctuations, quenched disorder, phase transitions, and transport in type-II superconductors" *Phys. Rev. B* **43** 130.

[3] M. Shahbazi, X. L. Wang, S. R. Ghorbani, M. Ionescu, O. V. Shcherbakova, F. S. Wells, A. V. Pan, S. X. Dou, K. Y. Choi (2013) "Vortex-glass phase transition and enhanced flux pinning in C^{4+}-irradiated $BaFe_{1.9}Ni_{0.1}As_2$ superconducting single crystals." *Supercond. Sci. Technol.* **26** 095014.

[4] D. J. Bishop, P. L. Gammel, C. A. Murray, D. B. Mitzi, A. Kapitulnik (1991) "Observation of an hexatic vortex glass in flux lattices of the high-T_c superconductor $Bi_2.1Sr_1.9Ca_0.9Cu_2O_{8+\delta}$" *Physica B* **169** 72-79.

[5] F. S. Wells, A. V. Pan, X. R. Wang,S. A. Fedoseev, H. Hilgenkamp (2015) Analysis of low-field isotropic vortex glass containing vortex groups in $YBa_2Cu_3O_{7-x}$ thin films visualized by scanning SQUID microscopy *Sci. Rep.* **5**, 8677.

[6] E. Kröner, K.-H. Anthony (1975) "DISLOCATIONS AND DISCLINATIONS IN MATERIAL STRUCTURES: The Basic Topological Concepts" *Annu. Rev. Mater. Sci.* **5** 43-72.

[7] S. Ryu, D. Stroud (1996) "First-order melting and dynamics of flux lines in a model for $YBa_2Cu_3O_{7-\delta}$" *Physical Review B* **54** 1320.

[8] J.R. Kirtley, J.P. Wikswo Jr. (1999) "Scanning SQUID microscopy" *Annu. Rev. Mater. Sci.* **29** 117.

[9] Ajay Nandgaonkar, D. G. Kanhere, Nandini Trivedi (2002) "Competition between columnar pins and vortex screening: A doubly reentrant phase diagram" *Phys. Rev. B* **66** 104527.

[10] V. Pan, *et al.*,(2006) "Supercurrent transport in $YBa_2Cu_3O_{7-\delta}$ epitaxial thin films in a dc magnetic field" *Phys. Rev. B* **73**, 054508.

[11] A. V. Pan, S. V. Pysarenko, S. X. Dou (2009) "Quantitative Description of Critical Current Density in YBCO Films and Multilayers" *IEEE Trans. Supercond.* **19** 3391.

[12] I. A. Golovchanskiy, A. V. Pan, O. V. Shcherbakova, S. A. Fedoseev (2013) "Rectifying differences in transport, dynamic, and quasi-equilibrium measurements of critical current density" *J. Appl. Phys.* **114** 163910.

[13] A. Sugimoto, T. Yamaguchi, I. Iguchi (2000) "Supercurrent distribution in high-Tc superconducting YBa2Cu3O7-y thin films by scanning superconducting quantum interference device microscopy" *Appl. Phys. Lett.* **77** 3069.

[14] I. A. Golovchanskiy, A. V. Pan, S. A. Fedoseev, M. Higgins, (2014) "Significant tunability of thin film functionalities enabled by manipulating magnetic and structural nano-domains", *Appl. Surf. Sci.* **311** 549.

[15] A. V. Pan, S. Pysarenko, S. X. Dou (2006) "Drastic improvement of surface structure and current-carrying ability in $YBa_2Cu_3O_7$ films by introducing multilayered structure" *Appl. Phys. Lett.* **88** 232506.

[16] A. V. Pan, S. V. Pysarenko, D. Wexler, S. Rubanov, S. X. Dou (2007) "Multilayering and Ag-Doping for Properties and Performance Enhancement in $YBa_2Cu_3O_7$ Films" *IEEE Trans. Appl. Supercond.* **17** 3585.

[17] A. V. Pan, Y. Zhao, M. Ionescu, S. X. Dou, V. A. Komashko, V. S. Flis, V. M. Pan (2004) "Thermally activated depinning of individual vortices in $YBa_2Cu_3O_7$ superconducting films *Physica C* **407** 1016.

[18] A. V. Pan, S. X. Dou (2006) "Comparison of small-field behavior in MgB_2, Low- and high-temperature superconductors" *Phys. Rev. B* **73**, 052506.

[19] Y. Tsuchiya, Y. Nakajima, T. Tamegai (2010) "Development of surface magneto-optical imaging method", *Phys. C* **470** 1123-1125.

[20] V. M. Pan and A. V. Pan, (2001) "Vortex matter in superconductors" *Fiz. Niz. Temp.* (Rus.) **27**, 991 [*Low Temp. Phys.* **27** 732 (2001)].

[21] C. Jooss *et al.* (2002) "Magneto-optical studies of current distributions in high-T_c superconductors" *Rep. Prog. Phys.* **65** 651.

[22] F. S. Wells (2011) "Magneto-optical imaging and current profiling on superconductors", Honours Thesis, University of Wollongong.

[23] B.J. Roth, N.G. Sepulveda, J.P. Wiskwo Jr. (1988) "Using a Magnetometer to Image a Two-Dimensional Current Distribution" *J. Appl. Phys.* **65** 361.

[24] A. V. Pan and P. Esquinazi, (2000) "The Labusch parameter of a driven flux line lattice in $YBa_2Cu_3O_7$ superconducting films", *Eur. Phys. J. B* **17** 405.

[25] A. V. Pan and P. Esquinazi, (2000) "Influence of a driving force on the pinning of a field-cooled vortex lattice", *Phys. C* **341-348** 1187.